Solid-State Electronics 198 (2022) 108455

Contents lists available at ScienceDirect

Solid State Electronics

journal homepage: www.elsevier.com/locate/sse

Ab initio study of electron mobility in V_2O_5 via polaron hopping☆

Remi Defrance [a,b,*], Benoit Sklénard [a,**], Marc Guillaumont [b], Jing Li [a], Michel Freyss [c]

[a] Univ. Grenoble Alpes, CEA, Leti, F-38000, Grenoble, France
[b] Lynred, 364 Avenue de Valence, 38113, Veurey-Voroize, France
[c] CEA, DES, IRESNE, DEC, Cadarache, 13108, Saint-Paul-lez-Durance, France

ARTICLE INFO

Keywords:
Polaron
DFT+U
V_2O_5
Trapping
Hopping
Mobility

ABSTRACT

We investigate the polaron transport in V_2O_5 using Density Functional Theory (DFT)+U. The Bond Distortion Method (BDM) is utilized to help stabilize an excess electron as a self-trapped polaron. The polaron hopping on a linearly interpolated pathway between two trapping sites is evaluated by Landau–Zener equations with parameters extracted using a model Hamiltonian and DFT ground state energies. The polaronic contribution of the electronic mobility is obtained from the Einstein relation and compared to experimental data. The influence of the Hubbard U correction used in DFT+U on both the polaron static and dynamic properties has also been studied.

1. Introduction

Vanadium pentoxide (V_2O_5) is a Transition Metal Oxide (TMO) that has received considerable attention in energy storage [18] or as a chemical catalysts [3] owing to its electrochemical properties. V_2O_5 thin films also show large Temperature Coefficients of Resistance (TCR) making them suitable for infrared detectors [1]. The TCR is one of the most important figures of merit of microbolometers [24]. It is defined as $\rho^{-1}d\rho/dT$ where ρ is the resistivity of the material and T the temperature. It is therefore essential to study the temperature dependence of the two key electronic transport quantities : carrier density and mobility.

The conduction mechanism in V_2O_5 has been found to be governed by small polaron hopping [12]. A polaron is an excess charge carrier that localizes on an atom or a group of atoms by coupling with a distortion of the lattice creating a polarization cloud [5]. They can be classified as small or large depending on the extension of the lattice distortion. In this work we focus on small polarons dynamics resulting from the transfer of the excess charge carrier between two trapping sites. The hopping transfer rates can be computed from first-principles calculations [4,11,17].

For materials such as V_2O_5 with strongly correlated d-orbitals, standard local and semi-local DFT calculations fail to predict the electronic properties. The main reason of this failure is the self-interaction error which can be circumvented by introducing an on-site Hubbard U correction for the $3d$ V electrons in the so-called DFT+U method. The value of U is usually determined empirically (e.g. adjusted to reproduce properties such as the band gap) even though it can be calculated with *ab initio* methods [19]. In this work, we investigate the impact of U on polaron properties, from its localization to its contribution to the electron mobility in V_2O_5.

2. Methods

All DFT+U calculations presented in this work are carried out using the PAW method implemented in the VASP code [8,9] and the Perdew–Burke–Ernzerhof (PBE) [15] exchange–correlation functional. To stabilize the polaron, we employ a 168-atoms supercell of orthorhombic V_2O_5 (spacegroup *Pmmn*) shown in Fig. 1 and we apply the Bond Distortion Method (BDM) with an initial distortion of 15% around one of the V atoms to localize the excess electron before relaxation. We use the Linear Interpolation (LI) method to simulate the polaron hopping. The coordinates of all the atoms along the hopping path are approximated as: $\mathbf{R} = x\mathbf{R_A} + (1-x)\mathbf{R_B}$, where $\mathbf{R_A}$ and $\mathbf{R_B}$ are the initial and final coordinates and x varies from 0 to 1. It should be noted that the excess electron introduces spurious interactions between the polaron and its periodic images that could impact the computed energy barriers [6]. However, in our case the charge remains localized along the hopping path meaning that these finite-size effects should cancel out.

Key transport parameters are usually computed using constrained Density Functional Theory (cDFT) to create diabatic states [11]. In this work, we employ an alternative method consisting in extracting the

☆ The review of this paper was arranged by Francisco Gamiz .

* Corresponding author at: Lynred, 364 Avenue de Valence, 38113, Veurey-Voroize, France.
** Corresponding author.
E-mail addresses: remi.defrance@lynred.com (R. Defrance), benoit.sklenard@cea.fr (B. Sklénard).

https://doi.org/10.1016/j.sse.2022.108455

Available online 23 September 2022

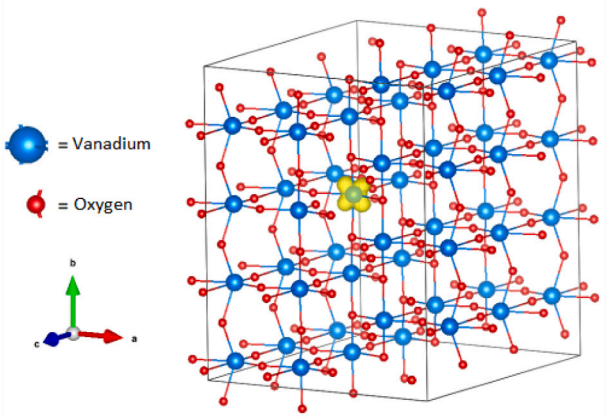

Fig. 1. Relaxed supercell of orthorhombic V_2O_5 with the charge density isosurface of the polaron (yellow) localized on a V atom. (For interpretation of the references to colour in this figure legend, the reader is referred to the web version of this article.)

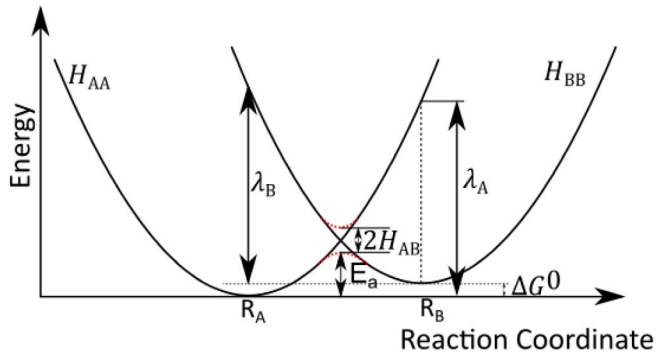

Fig. 2. Global description of the Marcus theory to describe the transition between two states. H_{AA} and H_{BB} are potential-energy surfaces of initial state A and final state B, H_{AB} is the coupling constant, E_a is the activation energy, λ_A and λ_B are the reorganization energies.
Source: Adapted from [4].

parameters from a fit of the adiabatic DFT total energy along the charge transfer pathway to a two-states model Hamiltonian:

$$\mathbf{H} = \begin{bmatrix} H_{AA} & H_{AB} \\ H_{BA} & H_{BB} \end{bmatrix} \tag{1}$$

with $H_{AA} = \lambda_A r^2 + E_{anhar}(r^3)$, $H_{BB} = \Delta G^0 + \lambda_B(1-r)^2 + E_{anhar}((1-r)^3)$ and $H_{AB} = H_{BA}$ the coupling constant. The harmonic contribution in the expression of H_{AA} and H_{BB} follows the Marcus theory [10] to describe the polaron transition from state A to state B as illustrated in Fig. 2. We also include an anharmonic contribution to improve the fit. Anharmonic behaviour of the hopping has been observed by calculating H_{AA} around $\mathbf{R}_A$ (as described before with x varying from −0.20 to 0.20). In this range H_{AA} is not a parabola and is correctly described with an additional anharmonic term.

Electronic mobilities were calculated based on the hopping rate obtained from the Landau–Zener equation [23]:

$$k_{ET} = \kappa_{el} \nu_{eff} \Gamma \exp\left(-\frac{E_a}{k_B T}\right) \tag{2}$$

with ν_{eff} the effective phonon frequency and:

$$\kappa_{el} = 2\frac{P_{LZ}}{1+P_{LZ}},$$

$$P_{LZ} = 1 - \exp\left(-\frac{\pi^{\frac{3}{2}} |H_{AB}|^2}{h\nu_{eff}\sqrt{\lambda_A k_B T}}\right)$$

Table 1
Properties of the polaron depending on the Hubbard U value : the formation energy (E_{POL}), the magnetic moment on the Vanadium atom with the localized electron (Magn.) and the crystal distortion around the polaron (Dist).

U (eV)	E_{POL} (eV)	Magn. (μB)	Dist. (%)
3.00	−0.10	0.992	3.74
3.25	−0.18	1.022	3.73
3.50	−0.26	1.045	4.07
4.00	−0.44	1.082	4.33
4.50	−0.64	1.112	4.54
5.00	−0.87	1.138	4.73

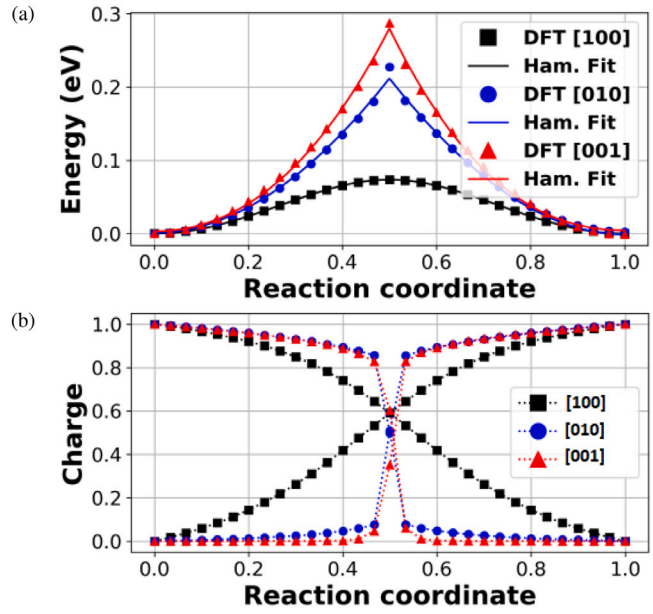

Fig. 3. Polaron hopping calculated with the LI method in the three main crystallographic directions with U=3.25 eV. (a) Hopping energy pathway and (b) Charge transfer during the hopping.

$\Gamma = 1$ the nuclear tunnelling factor, E_a the activation energy and ΔG^0 is the energy difference between state A and B. The polaron mobility is then evaluated from the Einstein relation:

$$\mu = \frac{|q|D}{k_B T}, \tag{3}$$

with $D = R^2 n_{neigh} k_{ET}$ where q is the charge of the carrier, R is the distance between the two sites and n_{neigh} is the number of neighbouring sites.

3. Polaron stabilization and hopping

We first stabilized the polaron with the BDM and obtained results in agreement to the literature [13,22]. We also confirm in Table 1 that the value of U has a significant impact on the polaron properties [16]. An increase of U leads to a decrease of the polaron formation energy (E_{POL}) as defined in [17], and an increase of the magnetic moment (Magn.) and of the lattice distortion around the polaron (average bond distortion of the 6 nearest neighbours), enhancing the stabilization of the polaron. Then, we simulate the hopping of the polaron along the [100], [010] and [001] directions using the LI method for U=3.25 eV. This value is used in the literature for V_2O_5 [20] and was determined by matching the oxydation energy and properties like the band gap of Vanadium Oxide [21]. The calculated barriers and energy pathways are anisotropic (according to crystallographic directions) as shown in Fig. 3. The calculated barriers in the three main crystallographic directions are also very close to other results in the literature [13].

Table 2
Electronic transport parameters extracted from the fit to the model Hamiltonian 1 for different Hubbard U values and crystallographic directions : E_a is the activation energy of the Landau–Zener model (E_a^{DFT} is obtained from DFT+U and E_a^{Ham} is the fit to the model Hamiltonian), H_{AB} is the coupling constant, k_{ET} is the transfer rate calculated at 300 K and μ is the mobility calculated at 300 K using the Einstein relation.

U (eV)	Direction	E_a^{DFT} (eV)	E_a^{Ham} (eV)	H_{AB} (eV)	k_{ET} (Hz)	μ (cm^2 V^{-1} s^{-1})
3.25	[100]	0.07	0.07	1.40×10^{-1}	5.82×10^{11}	5.5×10^{-2}
	[010]	0.23	0.22	5.90×10^{-5}	1.64×10^{4}	1.6×10^{-9}
	[001]	0.29	0.28	5.39×10^{-7}	1.08×10^{-1}	1.4×10^{-14}
4.00	[100]	0.14	0.14	1.10×10^{-1}	4.25×10^{10}	4.0×10^{-3}
	[010]	0.26	0.26	4.20×10^{-6}	1.28×10^{1}	1.3×10^{-12}
	[001]	0.30	0.30	1.00×10^{-5}	1.34×10^{1}	1.7×10^{-12}
5.00	[100]	0.23	0.23	6.00×10^{-2}	1.14×10^{9}	1.1×10^{-4}
	[010]	0.30	0.30	1.03×10^{-3}	1.34×10^{5}	1.3×10^{-8}
	[001]	0.34	0.34	4.36×10^{-3}	4.63×10^{5}	5.8×10^{-8}

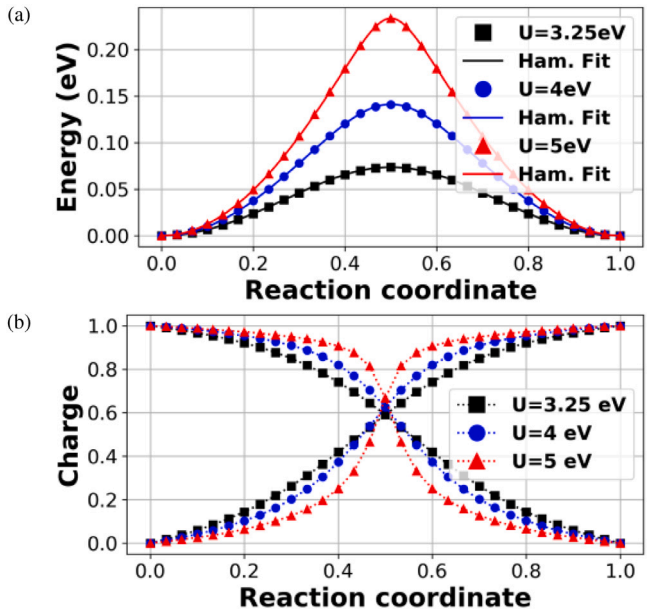

Fig. 4. (a) Polaron hopping energy barrier calculated using the LI method with U=3.25 eV (black), U=4 eV (blue) and U=5 eV (red) in the [100] direction. Markers are DFT data and lines are fit to the model Hamiltonian 1. (b) Charge transfer during the hopping along the [100] direction with the LI method with U=3.25 eV(black), U=4 eV (blue) and U=5 eV (red). (For interpretation of the references to colour in this figure legend, the reader is referred to the web version of this article.)

As we fit the Hamiltonian (Eq. (1)) to the DFT results, the shape of the energy curve directly affects the value of the extracted parameters reported in Table 2. According to the values of the λ_A/H_{AB} ratio, the hopping in the [100] direction is considered adiabatic while the hopping in the two other directions is considered nonadiabatic [4,10]. We can confirm this observation by looking at the charge transfer along the hopping path shown on Fig. 3. In the [100] direction the charge follows the displacement (adiabatic behaviour) while in the [010] and [001] ones the charge is transferred from site A to B near the saddle point (nonadiabatic behaviour).

Moreover, we show on Fig. 4 that as U increases, the barrier also increases. This behaviour is consistent with the influence of U on polaron properties shown in Table 2. The more the polaron is localized, the higher the barrier is for the polaron to hop from state A to state B. Furthermore, we also notice in Fig. 4 that the increase of U changes the energy pathway of the barrier and the hopping dynamics. As U increases, the [100] hopping becomes more and more nonadiabatic as the energy pathway looks more sharp and the localized electron follows less the reaction coordinate.

4. Polaron mobilities in crystalline V_2O_5

To compute the polaron mobility, we consider only nearest neighbours for the hopping and we use $\nu_{eff} = 10^{13}$ Hz which is a typical value for TMO [14]. The reported experimental mobility values measured at room temperature in V_2O_5 are scattered and range from 1.84×10^{-2} cm^{2}V^{-1}s^{-1} [2] to 4.75 cm^{2}V^{-1}s^{-1} [7]. The calculated mobility depends on the hopping direction and the value of U as shown in Table 2. The mobility ($\mu = 5.5\times10^{-2}$ cm^{2}V^{-1}s^{-1}) along the [100] direction, computed with U=3.25 eV, is close to the value reported in [2]. Other directions and higher values of U give smaller mobilities which means that the hopping along the [100] direction is dominant. Results of Table 2 also illustrate the strong dependence on the U value as the mobility is shifted by several orders of magnitude with a change of only 1 eV of U.

5. Conclusion

We investigated the static and the transport properties of polaron in monocrystalline V_2O_5 starting from an ab initio DFT+U method. We extracted polaron hopping parameters by mapping the DFT ground-state energies on the reaction coordinates to a model Hamiltonian. With the methodology adopted in this study we emphasize the sensitivity to the choice of the Hubbard U value, from the polaron self-trapping to its mobility. With U=3.25 eV (taken from Ref. [21] to reproduce experimental oxidation energies), the computed mobility is in good agreement with some of the experimental data reported in the literature. However, it is difficult to attribute experimentally one exact value of the electronic mobility for monocrystalline V_2O_5, because of its sensitivity to defects (such as oxygen vacancies) during the fabrication process. Moreover computed mobility diverge a lot regarding to the crystallographic direction. Therefore this methodology based on a fit to the model Hamiltonian needs further investigations.

Declaration of competing interest

The authors declare that they have no known competing financial interests or personal relationships that could have appeared to influence the work reported in this paper.

Data availability

Data will be made available on request.

References

[1] Awad ES, Al-Khalli N, Abdel-Rahman M, Alduraibi M, Debbar N. Comparison of V_2O_5 microbolometer optical performance using NiCr and Ti thin-films. IEEE Photon. Technol. Lett. 2015;27(5):462–5. http://dx.doi.org/10.1109/LPT.2014.2377203, URL http://ieeexplore.ieee.org/document/6975041/.

[2] Badot JC, Mantoux A, Baffier N, Dubrunfaut O, Lincot D. Electrical properties of V_2O_5 thin films obtained by atomic layer deposition (ALD). J. Mater. Chem. 2004;14(23):3411. http://dx.doi.org/10.1039/b410324f, URL http://xlink.rsc.org/?DOI=b410324f.

[3] Bond GC, Tahir SF. Vanadium oxide monolayer catalysts Preparation, characterization and catalytic activity. Appl. Catal. 1991;71(1):1–31. http://dx.doi.org/10.1016/0166-9834(91)85002-D, URL https://linkinghub.elsevier.com/retrieve/pii/016698349185002D.

[4] Deskins NA, Dupuis M. Electron transport via polaron hopping in bulk TiO_2 : A density functional theory characterization. Phys. Rev. B 2007;75(19):195212. http://dx.doi.org/10.1103/PhysRevB.75.195212, URL https://link.aps.org/doi/10.1103/PhysRevB.75.195212.

[5] Emin D. Polarons. Cambridge ; New York: Cambridge University Press; 2013.

[6] Freysoldt C, Grabowski B, Hickel T, Neugebauer J, Kresse G, Janotti A, Van de Walle CG. First-principles calculations for point defects in solids. Rev. Modern Phys. 2014;86(1):253–305. http://dx.doi.org/10.1103/RevModPhys.86.253, URL https://link.aps.org/doi/10.1103/RevModPhys.86.253.

[7] Haemers J, Baetens E, Vennik J. On the electrical conductivity of V_2O_5 single crystals. Phys. Stat. Sol. (A) 1973;20(1):381–6. http://dx.doi.org/10.1002/pssa.2210200140, URL https://onlinelibrary.wiley.com/doi/10.1002/pssa.2210200140.

[8] Kresse G, Furthmüller J. Efficient iterative schemes for ab initio total-energy calculations using a plane-wave basis set. Phys. Rev. B 1996;54(16):11169–86. http://dx.doi.org/10.1103/PhysRevB.54.11169.

[9] Kresse G, Joubert D. From ultrasoft pseudopotentials to the projector augmented-wave method. Phys. Rev. B 1999;59(3):1758–75. http://dx.doi.org/10.1103/PhysRevB.59.1758.

[10] Marcus RA. Electron transfer reactions in chemistry. Theory and experiment. Rev. Modern Phys. 1993;65(3):599–610. http://dx.doi.org/10.1103/RevModPhys.65.599, URL https://link.aps.org/doi/10.1103/RevModPhys.65.599.

[11] Melander M, Jónsson EÖ, Mortensen JJ, Vegge T, García Lastra JM. Implementation of constrained DFT for computing charge transfer rates within the projector augmented wave method. J. Chem. Theory Comput. 2016;12(11):5367–78. http://dx.doi.org/10.1021/acs.jctc.6b00815, URL https://pubs.acs.org/doi/10.1021/acs.jctc.6b00815.

[12] Murawski L, Gledel C, Sanchez C, Livage J, Audières J. Electrical conductivity of V_2O_5 and $Li_xV_2O_5$ amorphous thin films. J. Non-Crystalline Solids 1987;89(1–2):98–106. http://dx.doi.org/10.1016/S0022-3093(87)80324-1, URL https://linkinghub.elsevier.com/retrieve/pii/S0022309387803241.

[13] Ngamwongwan L, Fongkaew I, Jungthawan S, Hirunsit P, Limpijumnong S, Suthirakun S. Electronic and thermodynamic properties of native point defects in V_2O_5 : a first-principles study. Phys. Chem. Chem. Phys. 2021;23(19):11374–87. http://dx.doi.org/10.1039/D0CP06002J, URL http://xlink.rsc.org/?DOI=D0CP06002J.

[14] Pal S, Banerjee A, Chatterjee P, Chaudhuri BK. Evidence of non-adiabatic small polaron hopping conduction in $Bi_{0.1}A_{0.9}MnO_3$ (A=Ca, Sr, Pb). Phys. Stat. Sol. (B) 2003;237(2):513–22. http://dx.doi.org/10.1002/pssb.200301659, URL http://doi.wiley.com/10.1002/pssb.200301659.

[15] Perdew JP, Burke K, Ernzerhof M. Generalized gradient approximation made simple. Phys. Rev. Lett. 1996;77(18):3865–8. http://dx.doi.org/10.1103/PhysRevLett.77.3865, URL https://link.aps.org/doi/10.1103/PhysRevLett.77.3865.

[16] Reticcioli M, Diebold U, Franchini C. Modeling polarons in density functional theory: lessons learned from TiO_2. J. Phys.: Condens. Matter 2022;34(20):204006. http://dx.doi.org/10.1088/1361-648X/ac58d7, URL https://iopscience.iop.org/article/10.1088/1361-648X/ac58d7.

[17] Reticcioli M, Diebold U, Kresse G, Franchini C. Small polarons in transition metal oxides. In: Handbook of Materials Modeling. Cham: Springer; 2019, p. 1–39. http://dx.doi.org/10.1007/978-3-319-50257-1_52-1,

[18] Sathiya M, Prakash AS, Ramesha K, Tarascon JM, Shukla AK. V_2O_5 carbon nanotubes for enhanced electrochemical energy storage. J. Am. Chem. Soc. 2011;133(40):16291–9. http://dx.doi.org/10.1021/ja207285b, URL https://pubs.acs.org/doi/10.1021/ja207285b.

[19] Shih B-C, Abtew TA, Yuan X, Zhang W, Zhang P. Screened Coulomb interactions of localized electrons in transition metals and transition-metal oxides. Phys. Rev. B 2012;86(16):165124. http://dx.doi.org/10.1103/PhysRevB.86.165124, URL https://link.aps.org/doi/10.1103/PhysRevB.86.165124.

[20] Szymanski N, Liu Z, Alderson T, Podraza N, Sarin P, Khare S. Electronic and optical properties of vanadium oxides from first principles. Comput. Mater. Sci. 2018;146:310–8. http://dx.doi.org/10.1016/j.commatsci.2018.01.048, URL https://linkinghub.elsevier.com/retrieve/pii/S0927025618300612.

[21] Wang L, Maxisch T, Ceder G. Oxidation energies of transition metal oxides within the GGA + U framework. Phys. Rev. B 2006;73(19):195107. http://dx.doi.org/10.1103/PhysRevB.73.195107, URL https://link.aps.org/doi/10.1103/PhysRevB.73.195107.

[22] Watthaisong P, Jungthawan S, Hirunsit P, Suthirakun S. Transport properties of electron small polarons in a V_2O_5 cathode of Li-ion batteries: a computational study. RSC Adv. 2019;9(34):19483–94. http://dx.doi.org/10.1039/C9RA02923K, URL http://xlink.rsc.org/?DOI=C9RA02923K.

[23] Wu F, Ping Y. Combining Landau–Zener theory and kinetic Monte Carlo sampling for small polaron mobility of doped $BiVO_4$ from first-principles. J. Mater. Chem. A 2018;6(41):20025–36. http://dx.doi.org/10.1039/C8TA07437B, URL http://xlink.rsc.org/?DOI=C8TA07437B.

[24] Yadav PK, Yadav I, Ajitha B, Rajasekar A, Gupta S, Ashok Kumar Reddy Y. Advancements of uncooled infrared microbolometer materials: A review. Sensors Actuators A 2022;342:113611. http://dx.doi.org/10.1016/j.sna.2022.113611, URL https://linkinghub.elsevier.com/retrieve/pii/S0924424722002497.